W. L. HEITZ
Shell Development Company,
Emeryville, Calif.

J. W. WESTWATER
Professor of Chemical Engineering,
University of Illinois,
Urbana, Ill.
Mem. ASME

Critical Rayleigh Numbers for Natural Convection of Water Confined in Square Cells With L/D From 0.5 to 8

An experimental study of heat transfer modes in water heated from below was conducted using test cells of square cross section, 0.5 × 0.5 in., and heights of 1.25 to 4 in. Heat transfer was unidirectional and parallel to gravity. Tests both included and excluded the maximum density region of 4 deg C. Ice was present above the liquid during certain runs. The three modes of heat transfer, conduction and laminar and turbulent natural convection, were characterized by temperature profiles, fusion-front velocities and positions, and fluid flow patterns. Transitions between modes occur at well-defined critical Rayleigh numbers which are distinct functions of the L/D of the liquid. The critical values are not affected by the presence of ice, motion of the fusion front, or the temperatures of the warm and cold boundaries, if the Rayleigh number is calculated as described. The L/D was varied from 0.5 to 8 and the critical Rayleigh numbers varied from about 1700 to 10^8.

Introduction

THE EFFECT of boundary geometry, boundary temperature, and boundary motion on the modes of heat transfer in confined liquids is of wide interest. Possible applications include heat storage in space vehicles, the solidification of castings, crystal growth, and the circulation of liquids in tanks. Bénard [1][1] and Rayleigh [2], working with unbounded systems, were the first to study natural convection.

Studies of the effect of boundary dimensions on the transition between modes of heat transfer have been limited principally to the transition from pure conduction to laminar natural convection. This occurs under conditions which are defined herein as the first critical Rayleigh number, Ra_{c1}.

A mathematical model predicting Ra_{c1} for particular boundary configurations was presented by Ostrach and Pnueli [3]. Sherman and Ostrach [4] mathematically determined that for an arbitrary region $Ra_{c1} > 1558\ (L/d)$ where L is the vertical liquid dimension and d is the diameter of an equal-volume sphere. Finite-difference methods were used by Samuels and Churchill [5] to show that $Ra_{c1} = f\ (Pr, L/D)$, for $^1/_3 \leq L/D \leq 2$, where D is the horizontal liquid dimension. Edwards and Catton [6] and Edwards [7] presented mathematical models to predict Ra_{c1} with respect to L/D and cell-wall conductance.

[1] Numbers in brackets designate References at end of paper.

Contributed by the Heat Transfer Division and presented at the Winter Annual Meeting, New York, N. Y., November 29–December 3, 1970, of THE AMERICAN SOCIETY OF MECHANICAL ENGINEERS. Manuscript received by the Heat Transfer Division March 23, 1970; revised manuscript received July 8, 1970. Paper No. 70-WA/HT-7.

Nomenclature

C = liquid heat capacity, (cal)(gm)$^{-1}$ (deg C)$^{-1}$
D = horizontal dimension of square test cell, cm
E = vertical dimension of test cell, cm
Gr = Grashof number, dimensionless
g = acceleration of gravity, (cm)(sec)$^{-2}$
k = thermal conductivity, (cal)(sec)$^{-1}$ (cm)$^{-1}$(deg C)$^{-1}$
L = vertical dimension of liquid, cm
Pr = Prandtl number, dimensionless
Ra = Rayleigh number, dimensionless
T = temperature, deg C
ΔT = temperature difference, deg C
Δx = significant vertical length, cm
β = liquid coefficient of expansion, (deg C)$^{-1}$
ϵ = ice thickness, cm
μ = liquid viscosity, (gm)(cm)$^{-1}$ (sec)$^{-1}$
ρ = liquid density, (gm)(cm)$^{-3}$

Subscripts

a = lower boundary
b = upper boundary
$c1$ = critical value between pure conduction and laminar natural convection
$c2$ = critical value between laminar and turbulent natural convection
1 = solid phase
2 = liquid phase

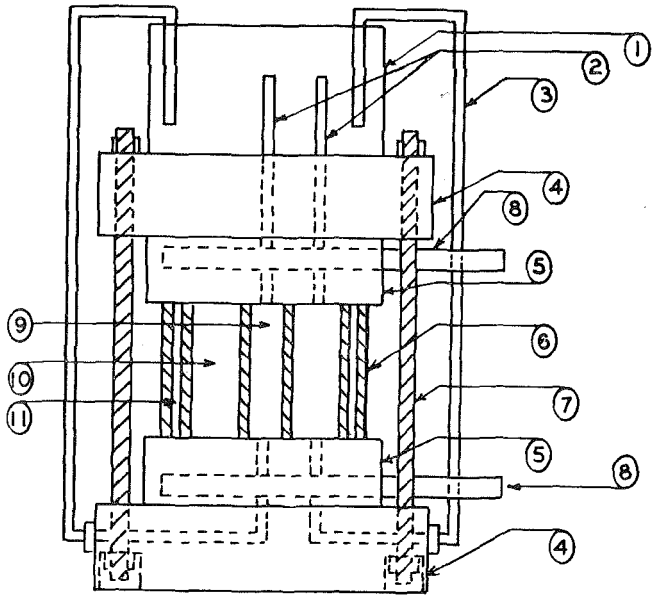

Fig. 1 Front view of test cell

The model of Davis [8] appears to be the most rigorous. Linear stability theory is used to predict Ra_{c1} as a function of L/D for enclosed fluids with both square and rectangular horizontal cross section, for conducting walls, and for $^1/_6 \leq L/D \leq 4$.

Experimental Ra_{c1} were presented by Schmidt and Silveston [9] for $L/D < 0.1$ and by Catton and Edwards [10] for $0 < L/D \leq 2.5$.

There have been no models presented which will predict the transition between laminar and turbulent natural convection. In this paper, this second crisis is defined by means of a second critical Rayleigh number, Ra_{c2}. Schmidt and Silveston presented an experimental value for test conditions with $L/D < 0.1$.

The object of the present study was to define the three modes of heat transfer, in terms of experimental measurements, and to determine values of the Rayleigh numbers at the transition points. Variables included the liquid depth, boundary temperatures, and motion of one boundary.

Apparatus and Procedure

The test assembly is illustrated in Fig. 1. All test measurements were taken in the center chamber of three concentric square tubes having inside dimensions in the horizontal plane of 0.5 × 0.5 in., 2.25 × 2.25 in., and 2.875 × 2.875 in. Three nominal heights were used: 1.25, 2.0, and 4.0 in. The walls were of 0.125-in-thick polymethylmethacrylate transparent plastic. The test liquid, distilled deaerated water, was present in the center chamber and in the first surrounding guard region. This water-filled guard region, the next surrounding guard region (filled with air), and 3 in. of glass wool surrounding the test assembly insured one-dimensional heat transfer in the center chamber (to within a maximum error of 5 percent). For certain tests described later, for which the error would have exceeded 5 percent with the above arrangement, the two outer plastic tubes were removed and replaced with 6 in. of glass wool. This resulted in one-dimensional heat transfer again within 5 percent.

Heat sources and sinks were located at the top and bottom of the test assembly. These were constructed of 3.44 × 3.44 × 1.00 in. copper blocks. Grooves of 0.156-in. depth were milled in one surface of each copper block to accommodate the test section. The test section was sealed in the grooves with silicone rubber and held by tie rods.

The temperature of each copper block was controlled by passing methanol at various temperatures through the fluid flow passages. A series of constant-temperature baths (dry ice–Freon-11, ice water–salt, ice water, tap water, and tap water–steam) and pumps and heating tapes controlled by Variacs allowed temperatures in either copper block to be maintained at from −50 to +50 deg C and to within 0.1 deg C for over 2 hr.

To accommodate volume changes and eliminate the resultant destructive pressures which occur during phase change, the top and bottom of the test and guard regions were connected to a liquid reservoir by $^1/_8$-in-dia vent tubes. An excess of water was maintained in the liquid reservoir during all runs. The actual intake or outflow of water during a run was small and had no important effect on heat transfer inside the test region.

Thermocouples (three or five, depending on the cell height) of 0.005-in. duplex copper–constantan wires were inserted horizontally into the test region. The thermocouples were approximately equally spaced in a vertical direction and were located 0.06 in. from the back wall of the test region to minimize their possible influence on interfacial and fluid motion. The exact thermocouple spacings were determined with a cathetometer after each test cell had been assembled. Two additional thermocouples were located in the copper blocks near the top and bottom of the test region. Their temperatures were defined as the boundary temperatures of the test material. Temperatures were recorded using a 2-sec multi-point recorder and three single-point continuous recorders.

The test cell was mounted in one of three optical systems. The first, similar to one used by Thomas and Westwater [11], consisted of the test cell, a microscope, a camera, and a light source mounted on an optical bench. Time-lapse photography of motion of the fusion front, at 1 frame every 1 or 2 sec and with a magnification on the negative of from 4.5 to 50×, was obtained using this system. The second and third optical systems were used to observe fluid flow patterns. The Schlieren system consisted of a light source, a slit, a knife edge, two 6-in-dia parabolic mirrors, and a camera. It was used to observe laminar and turbulent convective fluid motion and the transition between the two modes. The suspension system consisted of a light source, a slit, a 6-in-dia parabolic mirror, and a camera. It was used to view a suspension of polystyrene dust in water. The particles, of diameter less than 0.003 in., were present in a concentration of about 20 per cu cm of water. This third system was used to observe laminar convection, or the lack of motion (conduction), and the transition between the two modes. In the latter two systems, the two guard regions of the test assembly were replaced by 6 in. of glass wool. Motion pictures of the Schlieren patterns and suspended particles were obtained at 12 frames per sec with a 0.3× magnification on the negative. During photography or direct visual observations, a plug of insulation was removed from each side of the cell to provide an optical path. The time during which the insulation was open was short (about 15 sec) and had negligible effect on the heat transfer as indicated by temperature profiles.

The procedure consisted of loading and mounting the test cell, obtaining the desired boundary temperatures, and then recording

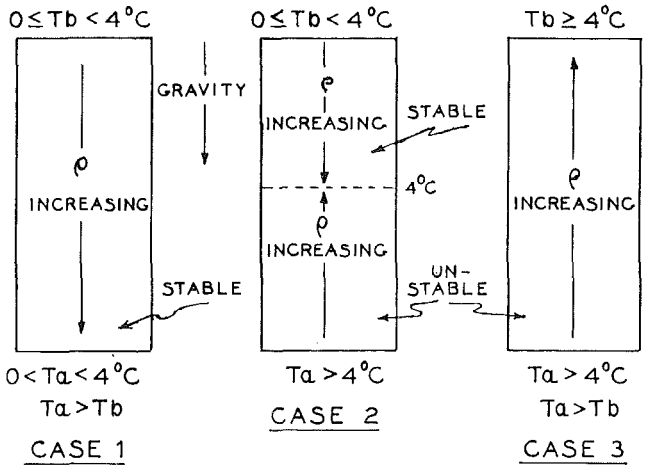

Fig. 2 Stability configurations for water heated from below

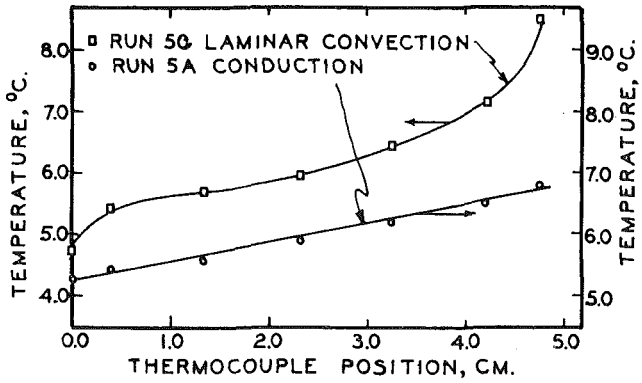

Fig. 3 Comparison of typical temperature profiles for conduction and for laminar natural convection in the liquid heated from below

temperatures, fusion-front motion, and liquid motion for both transient and steady-state conditions. Complete details of the apparatus and procedure are available [12].

Results and Discussion

Modes of Heat Transfer in the Liquid. When water, confined between parallel horizontal plates, is heated from below, three density configurations are possible as indicated in Fig. 2. The first two configurations are possible also with ice at the top, in which case $T_b < 0$ deg C. Case 1 is stable and heat transfer is by conduction only. If the density inversions in Cases 2 and 3 are very small, conduction is the mode of heat transfer. However, as the buoyancy forces are increased, laminar convection will arise. If the buoyancy driving force becomes sufficiently large, turbulent convection occurs.

Conduction. At steady state, the pure conduction region is characterized by a linear temperature profile along the vertical axis, as shown by the lower curve in Fig. 3. Deviations from linearity were less than 4 percent, and these were due to the recording accuracy. When both solid and liquid are present during conduction in the liquid, the Nusselt number is unity and

$$\frac{k_1 \Delta T_1 (E - \epsilon)}{k_2 \Delta T_2 \epsilon} = 1 \qquad (1)$$

During steady-state conduction, equation (1) was obeyed to within 5 percent. No motion could be detected when suspended particles were added. When ice was present, its interface was flat. If phase change was occurring (unsteady-state heat transfer), the interface was flat and its motion was continuous.

Laminar Natural Convection. Laminar natural-convection heat transfer is characterized by a smooth, nonlinear temperature profile along the vertical direction. The fluid motion is in the form of steady, cellular convection. A typical temperature profile is shown as the upper curve in Fig. 3.

The laminar region includes a multiple number of flow patterns. Fig. 4 shows the four patterns detected in the present tests. These were identified by examination of suspended particles. A selection of the motion pictures is available for loan [13]. The single-roll cell was always observed at the onset of convection and thus at low Rayleigh numbers. As the Rayleigh number was increased, this configuration was replaced by one of the three remaining configurations. For any particular value of L/D, configurations b and c were usually observed at lower Ra than was configuration d. The multiple-cell patterns occurred always as a vertical array. Presumably, the test cell was too narrow to permit a horizontal array of circulation cells.

In a small number of cases repetitive temperature oscillations were observed during laminar convection. Oscillations similar to those in Fig. 5*a* had amplitudes usually less than 0.5 deg C, existed for less than 10 min, and were recorded near steady-state conditions. The use of suspensions and also the use of Schlieren

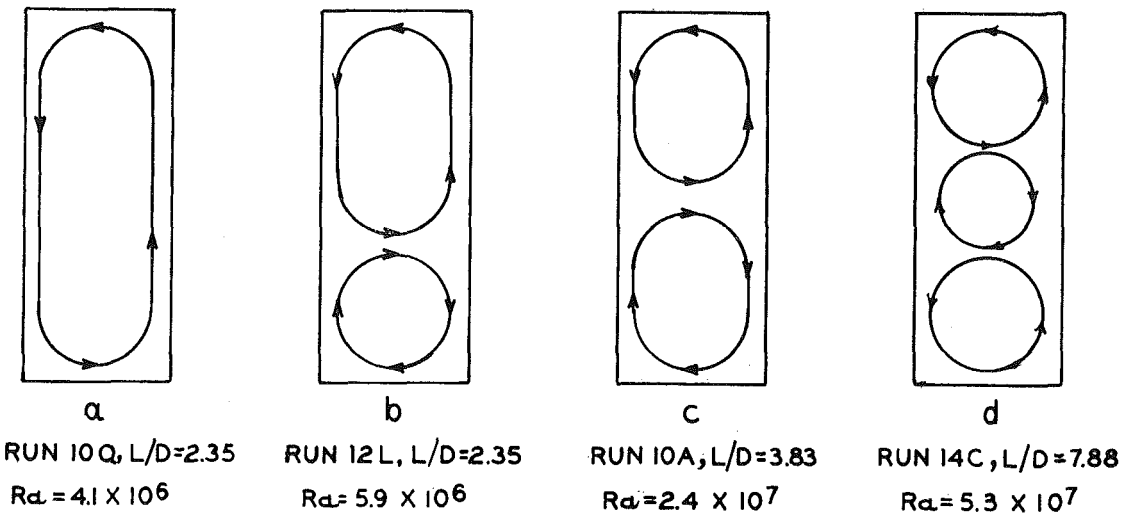

Fig. 4 Observed laminar natural convection flow patterns

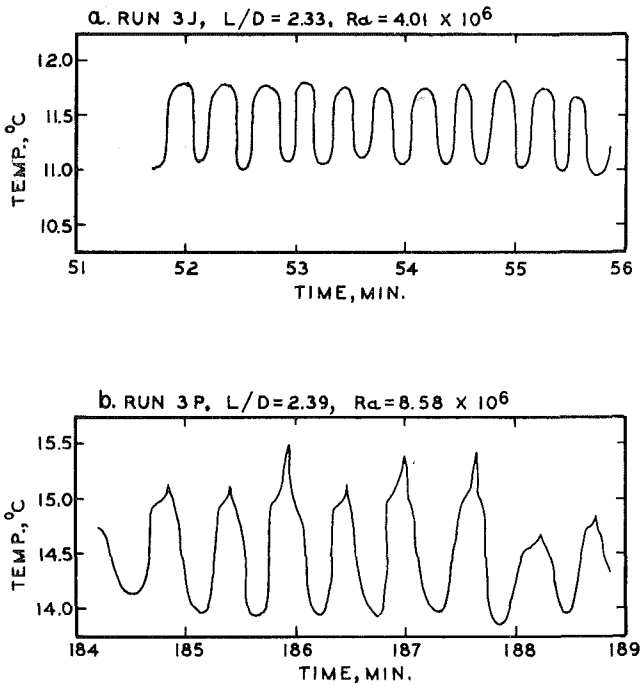

Fig. 5 Typical temperature oscillations recorded during laminar natural convection under certain conditions

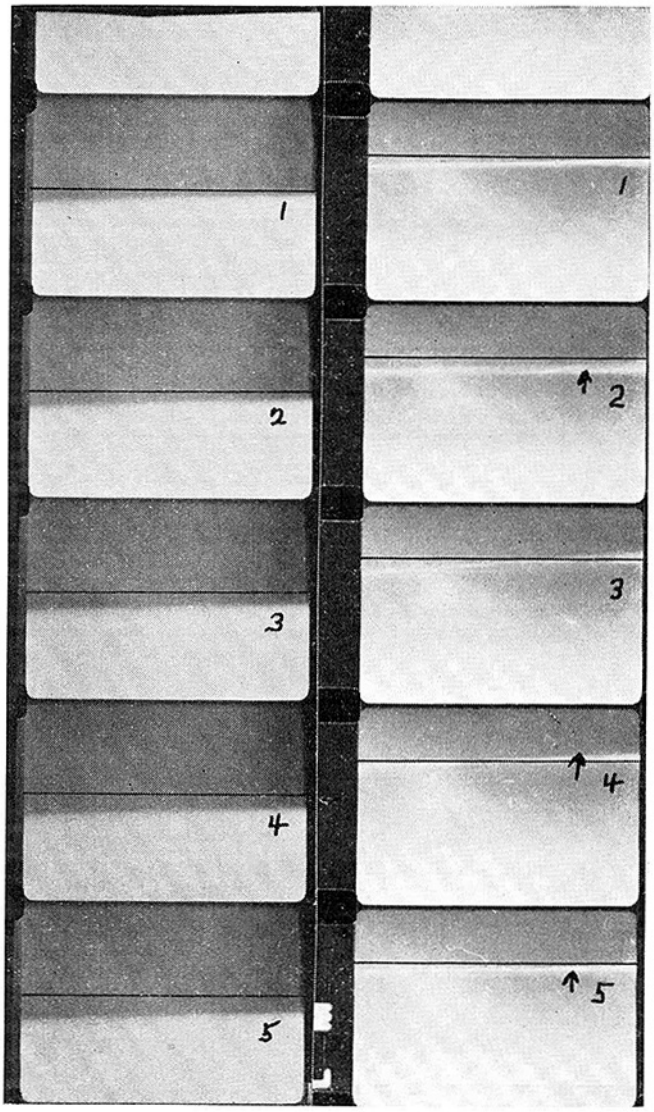

Fig. 6 Time-lapse motion pictures at 1 frame per 2 sec taken through a microscope showing motion of the fusion front during freezing; the width of the view is 0.090 in.; during laminar natural convection (left) the interface moves continuously away from the drawn reference line; during turbulent natural convection (right) the interface oscillates below (frame 2), above (frame 4), and below (frame 5) the reference line

illumination showed that these oscillations occurred during a transition from one flow configuration (in Fig. 4) to another, when the edge of a roll cell was at or near a thermocouple. During transition, the boundaries of the roll cells fluctuated up and down, passing the thermocouple. Similarly, oscillations shown in Fig. 5*b* occurred near the transition from laminar to turbulent convection. These lasted as long as an hour.

Phase change occurred during some tests with laminar convection. The motion of the fusion front was continuous as shown in Fig. 6. However, the interface was concave into the ice, in contrast to the conduction case. This is the result of the liquid flow pattern, such as in Fig. 4. The curvature of the interface was obvious in photographs at low magnification. It is not obvious at high magnification such as in Fig. 6.

Turbulent Natural Convection. A significant feature of turbulent natural convection is that the temperature at every thermocouple in the liquid becomes randomly oscillatory. This is illustrated in Fig. 7. The transition in the temperature profile was simultaneous with the transition from turbulent to laminar convective flow. Also shown in Fig. 7 is the temperature history of a thermocouple in the ice for the same run. The fact that the thermocouple in ice gave a flat temperature record indicates that the temperature oscillations observed with water are not caused by any equipment or background "noise."

Fig. 8 illustrates Schlieren photographs for both laminar and turbulent liquid convection. The laminar convective patterns are stationary. Their images are not as sharp as for the turbulent patterns since the density gradients are not as large. During turbulent convection the patterns are no longer stationary; random plumes of warm fluid rise and random plumes of cold liquid plunge in the bulk liquid. These plumes can be seen in the motion pictures [13].

During turbulence, boundary layers develop at both the top and bottom of the liquid. Viewed by Schlieren illumination, the upper cool layer is dark and is not as easily seen as the warm layer at the bottom. Plumes of warm liquid were observed to rise both from the surface of the copper block and from the interface between the bulk fluid and the warm boundary layer. The intermittent, irregular plumes caused the observed temperature oscillations and variations in the thickness of the boundary layers. Although the point temperatures in the liquid fluctuated, the time-average and space-average temperature in the liquid was constant.

Phase change occurred during some tests with turbulent convection. The motion of the water–ice interface frequently reversed direction. Thus, both melting and freezing occurred during a run having net melting (or net freezing). This erratic behavior is a result of the erratic fluid motion. The distance traveled during each reversal in the motion of the fusion front is microscopic. This is illustrated in Fig. 6. Oscillations of the water–ice interface were reported also by Boger and Westwater [14]. Oscillations of the interface cause an apparent large scatter in data for the fusion-front velocity. The magnitude of the scatter depends on the time increments selected for measurements of the position of the fusion front. The scatter seen in Fig. 9 is arbitrary in that sense. However, the scatter is a result of the physical phenomenon and is not due to experimental error.

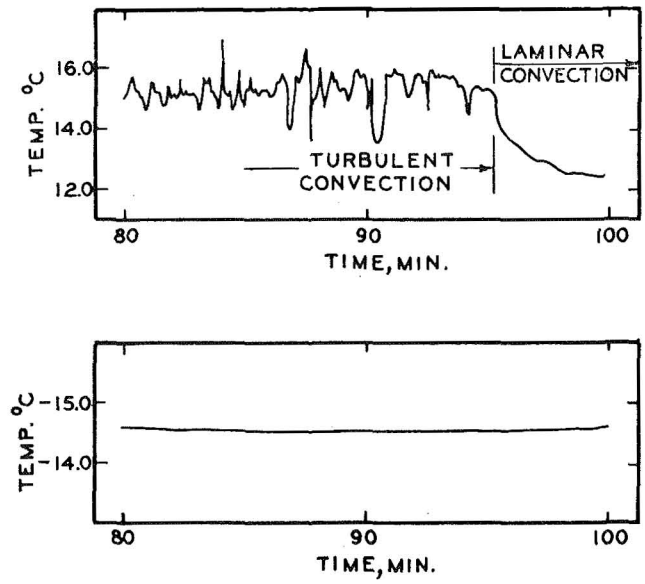

Fig. 7 Random temperature oscillations during turbulent natural convection followed by transition to laminar natural convection; the upper record is for a thermocouple in the liquid; the lower is for the solid; run 8E, $T_b = -36.4$ deg C, $T_a = 11.5$ deg C

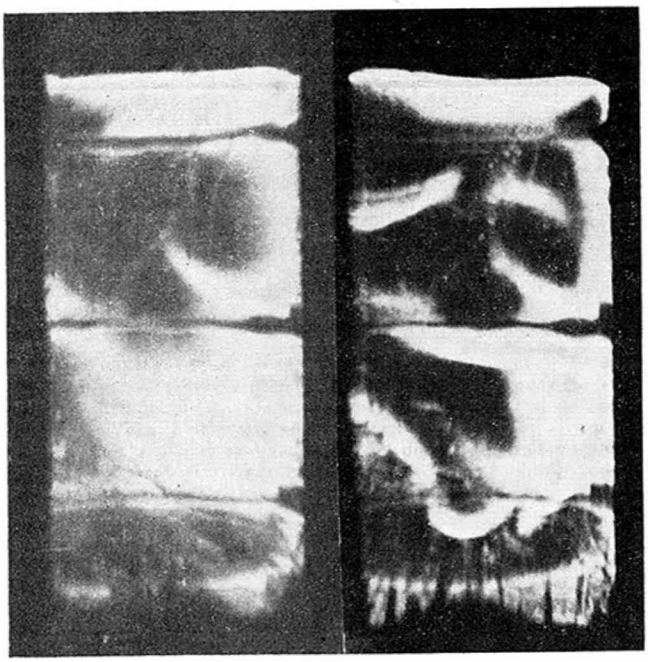

Fig. 8 Schlieren photographs of laminar (left) and turbulent (right) natural convection; the width of the view is 0.5 in.; the 3 horizontal wires are the thermocouples

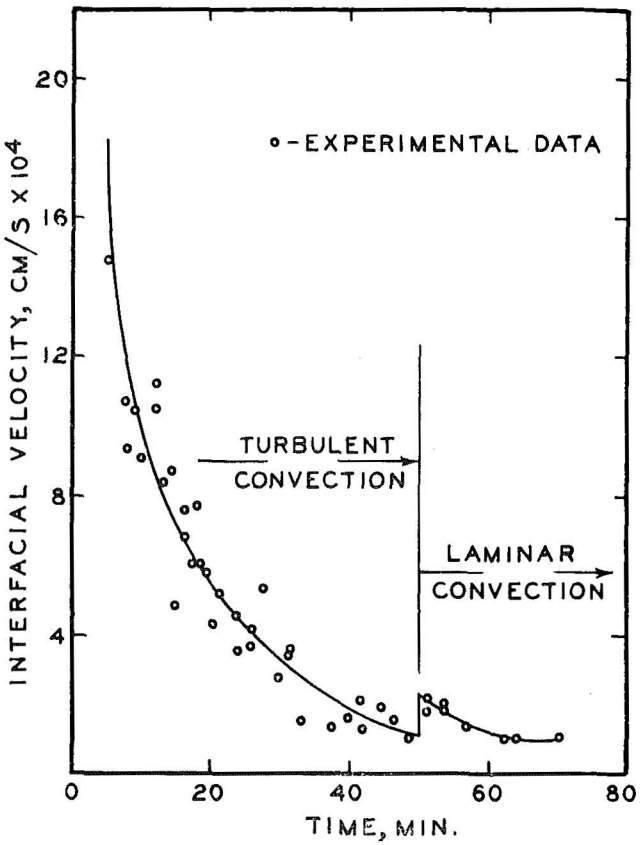

Fig. 9 Fusion-front velocity during transition from turbulent to laminar natural convection; run 3F, freezing of water at 24 deg C from the top by reducing the top temperature to −44 deg C

In Fig. 9 velocity data during turbulent and during laminar natural convection may be compared. The velocity of the fusion front increases at 50 min as the transition to laminar convection occurs. It is a general observation that an increase in convection reduces the rate of freezing and increases the rate of melting. A decrease in convection causes the opposite effects.

The magnitudes of the oscillations in the liquid temperature at a point and in the fusion-front velocity during turbulent convection are shown in Fig. 10. The amplitudes of the oscillations and their frequencies increase as the Rayleigh number increases. The largest temperature oscillation shown is about 3 deg C with a period of about 8 sec. The largest velocity oscillation was about 10^{-3} cm/sec and the period was about 14 sec.

Transitions Between Heat-Transfer Modes. Transitions from one heat-transfer mode to another were determined and the corresponding Rayleigh numbers were computed.

$$\mathrm{Ra} = \frac{\rho^2 g C \beta \Delta T \Delta x^3}{\mu k_2} \propto \frac{\text{buoyancy forces}}{\text{viscous forces}} \tag{2}$$

When water is used, the density maximum at 4 deg C complicates the selection of the physical properties, the liquid depth, and the temperature driving force. Boger and Westwater used empirical means to show the best selection, and their recommendations are used herein. Thus, when $T_a > T_b > 4$ deg C, water behaves as a normal fluid and one uses

$\Delta x = E - \epsilon$
$\Delta T = T_a - T_b$
ρ, C, μ, and k_2 are evaluated at $(T_a + T_b)/2$
β is evaluated at T_a

When the liquid contains the maximum-density region one uses

$\Delta x = E - \epsilon$
$\Delta T = T_a - 4$, deg C
ρ, C, μ, and k_2 are evaluated at $(T_a + 4)/2$, deg C
β is evaluated at T_a

The first critical Rayleigh number (onset of laminar convection) was identified by the temperature profiles, the water ice interface position, and the motion of suspended particles. The second critical Rayleigh number (onset of turbulent convection) was identified by temperature profiles, fusion-front velocity data as in Fig. 9, the motion of suspended particles, and the motion

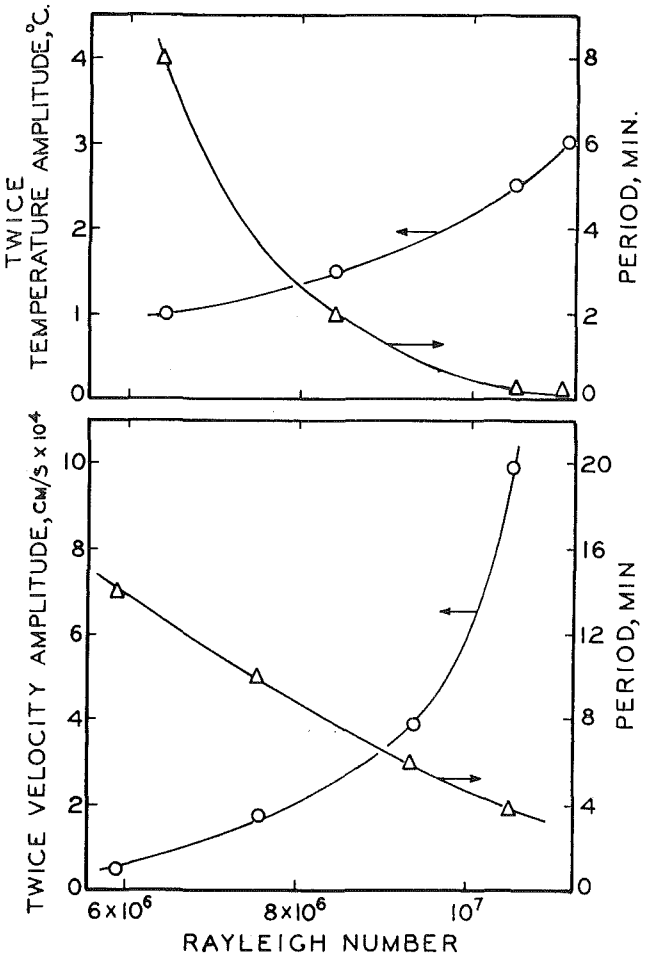

Fig. 10 Dependence of liquid temperature oscillations and fusion-front velocity oscillations on Rayleigh number

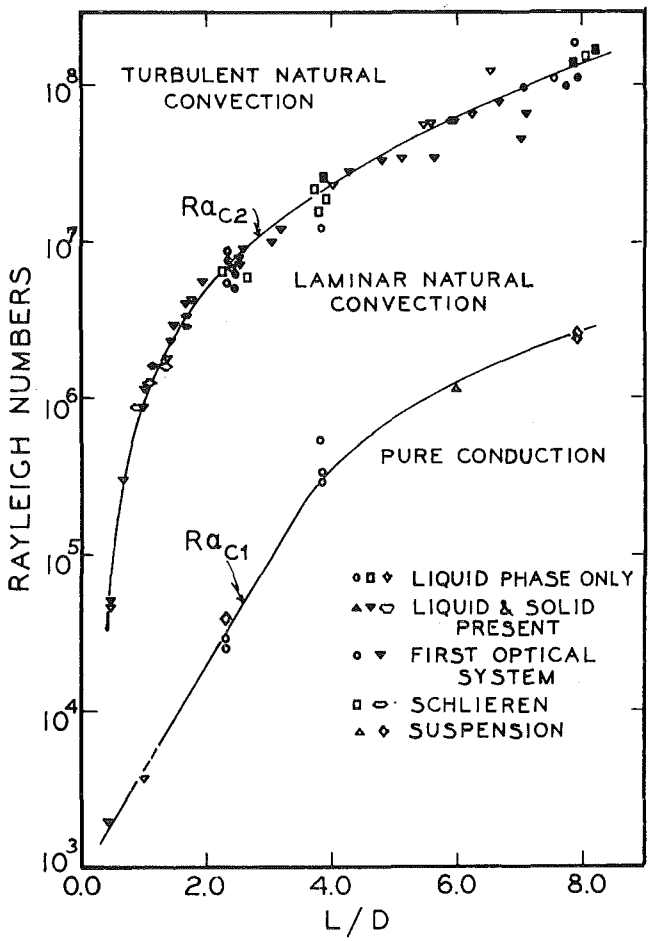

Fig. 11 Effect of L/D on the critical Rayleigh numbers for transitions between three modes of heat transfer; $D = 0.5$ in.; open symbols for Ra_{c2} are for transitions from laminar to turbulent convection; solid symbols are the reverse

visible by Schlieren illumination. Thus, three and four checks were used and the likelihood of a false judgment is remote.

Fig. 11 shows that the two critical Rayleigh numbers are functions of the liquid depth/width ratio, L/D. The lower curve (Ra_{c1}) separates the region of pure conduction from that of laminar convection, whereas the upper curve (Ra_{c2}) separates laminar convection from turbulent convection. Each point on the lower curve is the result of several steady-state runs approaching the transition from each side. The time to achieve steady state was 2 to 5 hr. The upper curve was determined at both steady-state and transient conditions, and again the approach was from both sides. For a given L/D, the range of the Rayleigh number over which a transition occurs is roughly 50 percent of the Rayleigh number. This bandwidth is a small magnitude for natural convective processes.

Also designated in Fig. 11 is the optical system used to obtain each data point. Scatter in the data obtained using the first optical system arose because liquid was present in both the test region and guard region of the test cell. Since the L/D in the guard region was less than the L/D in the test region, convection in the guard region may have been greater than in the test region. This could result in some horizontal temperature gradients. In the Schlieren and suspension studies, this possibility was eliminated, and the data scatter was small.

Although the moving boundary during phase change causes the L/D ratio to change, the results show that for any particular value of L/D, the values of the critical Rayleigh numbers are not affected by the presence of the solid phase nor by the presence of a moving boundary with a velocity of the order of 10^{-4} cm/sec.

The Rayleigh number, equation (2), is proportional to the ratio of buoyancy to viscous forces. Drag forces introduced at the boundaries are a function of the size and shape of the boundaries. Thus the effect of cell size may be expected to be a function of the ratio of total wetted area to liquid volume. For a cell of square cross section, this ratio is

$$M = \frac{\text{area}}{\text{volume}} = \frac{2}{D}\left[\frac{1}{L/D} + 2\right] \tag{3}$$

For small values of L/D, M is very sensitive to changes in L/D. For large values of L/D, M approaches the limit $4/D$ asymptotically and Ra_c should show less dependence on L/D. The data of Fig. 11 illustrate this relationship. For the largest L/D used in this work, 8.0, M was within about 6 percent of its limiting value. Note that $D = 0.5$ in. for all data in Fig. 11. The curves could be different for other values of D. Cases for which the maximum density region was both present and absent are included in Figs. 11 and 12. The results are consistent for both cases.

The results of this work are compared with those of other investigators in Fig. 13. The experimental data of Catton and Edwards [10] were obtained using silicone oil (Dow Corning, 50 and 100 cp) confined in cells of hexagonal cross section. Good agreement suggests that the Ra_c versus L/D correlations may be applicable to a wide range of liquids confined in cells of various cross sections. The results of Schmidt and Silveston [9] were obtained in thin fluid layers where $3 \leq Pr \leq 4 \times 10^3$, $10^{-1} \leq Gr \leq 8 \times 10^4$; the effect of L/D was not considered.

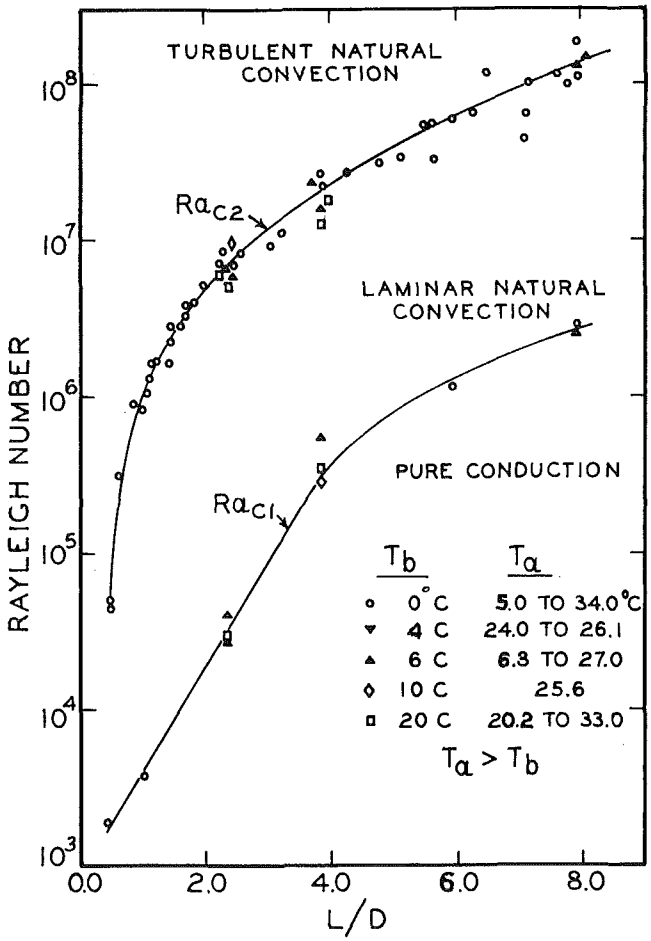

Fig. 12 Test for possible effect of boundary temperatures on the critical Rayleigh numbers; no effect is apparent

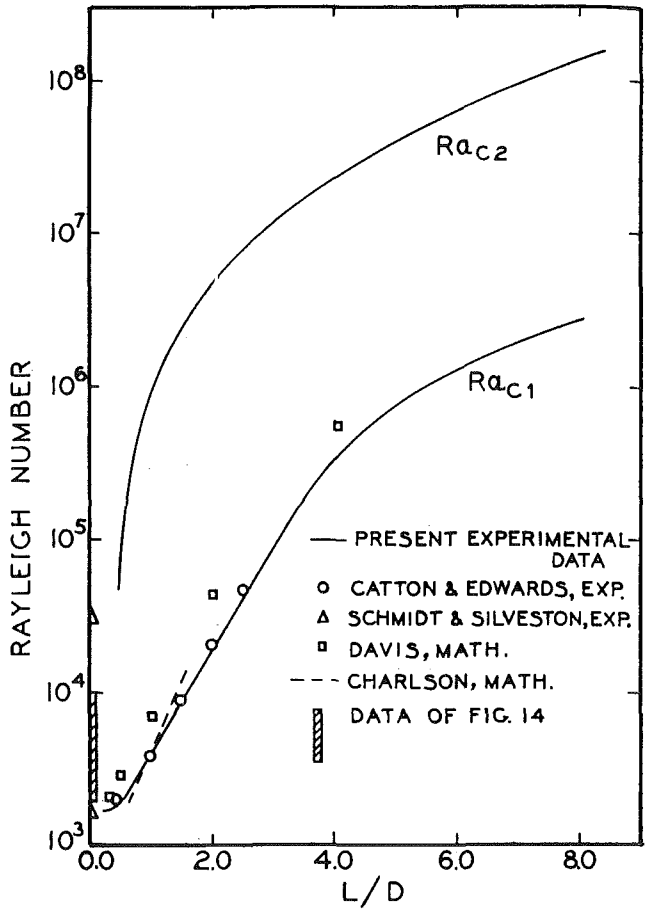

Fig. 13 Comparison of new data with results of other investigators

The mathematical results of Davis [8] were obtained for the same boundary conditions as used in this work except that Davis assumed the boundaries to be perfect conductors. The results lie above but parallel to those of this work. This is expected, because conducting walls transfer part of the energy and thereby reduce buoyancy forces. The results of Charlson and Sani for cylindrical cells [15] are in good agreement with the data; insulating boundaries were assumed in their mathematical model.

Yen [16] obtained the following experimental relationship:

$$\mathrm{Ra}_{c1} = 1.42 \times 10^4 \exp(-6.64 \times 10^{-2} T_s) \qquad (4)$$

where T_s is the lower surface temperature ($6.72 \leq T_s \leq 25.5$ deg C). This result indicates that the onset of convection is dependent only on T_s and is independent of L/D. The results of the present work do not agree with this conclusion. Yen's data replotted actually show a dependence of L/D on Ra_{c1} as shown in Fig. 14. In addition, the data do not agree with those of other investigators (see Fig. 13).

Tien [17] presents a mathematical model for Ra_{c1} also based on boundary temperatures only. His predicted results were shown to be in agreement with the data of Boger and Westwater. Unfortunately, the cell length in reference [14] had been rounded off to 2 in. (5.08 cm); the correct values varied from 4.75 to 5.07 cm. When correct values are used, the model of Tien fails to predict the transition. If the predicted results of Tien are plotted versus L/D as shown in Fig. 15, they disagree with the present data.

Tien and Yen state that the critical Rayleigh number for the onset of convection varies with the temperature of the heated boundary. This possibility was examined also in the present study. The results, Fig. 12, show no effect, nor does the temperature of the cold boundary affect the critical Rayleigh number. Note that four independent methods were used to detect the critical Rayleigh numbers in the present tests. Tien and Yen used one method only, the identification of a change in the slope of a graph.

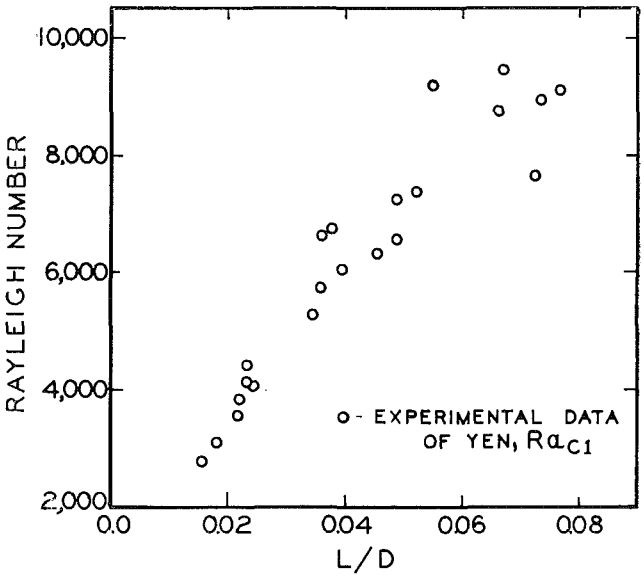

Fig. 14 Effect of L/D on Ra_{c1}; data of Yen

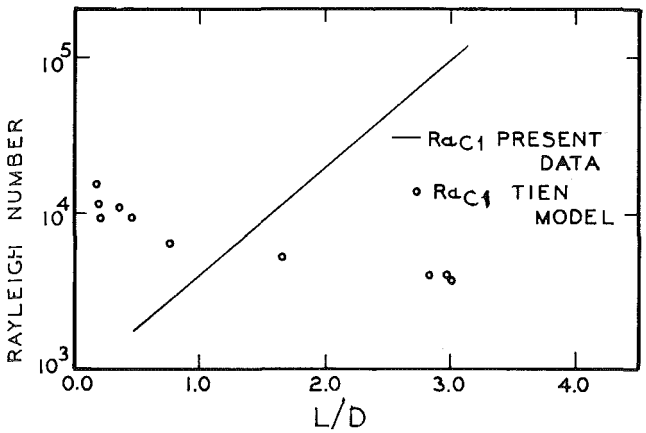

Fig. 15 Comparison of new data with results of Tien

Conclusions

1 An apparatus was developed which permitted the use of four independent methods to detect the three modes of one-dimensional heat transfer in water confined in a cell.

2 Transitions between heat-transfer modes were studied and the corresponding Rayleigh numbers were determined in the range 1700 to 10^8.

3 The critical Rayleigh numbers are strongly dependent on L/D in the range $0.5 < L/D < 8.0$.

4 The bandwidth of the transition region corresponds to a Rayleigh-number variation of about 50 percent.

5 The presence of ice at the top or a moving fusion front has negligible effect on the critical Rayleigh numbers.

6 The presence of the maximum density region does not affect the critical values, provided the physical properties and the temperature difference are selected as described.

7 The data agree with mathematical predictions by Davis, and by Charlson and Sani; they agree with data of Catton and Edwards, and Schmidt and Silveston; they disagree with the mathematical predictions by Tien and the experimental results of Yen.

Acknowledgment

A NASA Traineeship, a Dow Chemical Company Fellowship, and a National Science Foundation Grant supported this research.

References

1 Bénard, H., "Les tourbillons cellulaires dans une nappe liquide transport—aut de la chaleur par convection en régime permanent," *Ann. Chem. Phys.*, Vol. 23, 1901, pp. 62–144.

2 Lord Rayleigh, "On Convective Currents in a Horizontal Layer of Fluid When the High Temperature is on the Underside," *Philosophical Magazine*, Vol. 32, 1916, pp. 529–546.

3 Ostrach, S., and Pnueli, D., "The Thermal Instability of Completely Confined Fluids Inside Some Particular Configurations," JOURNAL OF HEAT TRANSFER, TRANS. ASME, Series C, Vol. 85, No. 4, Nov. 1963, pp. 346–354.

4 Sherman, M., and Ostrach, S., "Lower Bounds to the Critical Rayleigh Number in Completely Confined Regions," *Journal of Applied Mechanics*, Vol. 34, TRANS. ASME, Series E, Vol. 89, No. 2, June 1967, pp. 308–312.

5 Samuels, M. R., and Churchill, S. W., "Stability of a Fluid in a Rectangular Region Heated from Below," *AIChE Journal*, Vol. 13, No. 1, 1967, pp. 77–85.

6 Edwards, D. K., and Catton, I., "Prediction of Heat Transfer by Natural Convection in Closed Cylinders Heated from Below," *International Journal of Heat and Mass Transfer*, Vol. 12, 1969, pp. 23–30.

7 Edwards, D. K., "Suppression of Cellular Convection by Lateral Walls," JOURNAL OF HEAT TRANSFER, TRANS. ASME, Series C, Vol. 91, No. 1, Feb. 1969, pp. 145–150.

8 Davis, S. H., "Convection in a Box: Linear Theory," *Journal of Fluid Mechanics*, Vol. 30, Part 3, 1967, pp. 465–478.

9 Schmidt, E., and Silveston, P. L., "Natural Convection in Horizontal Liquid Layers," *Chem. Engr. Prog. Symp. Series*, Vol. 55, No. 29, 1959, pp. 163–169.

10 Catton, I., and Edwards, D. K., "Effect of Side Walls on Natural Convection Between Horizontal Plates Heated from Below," JOURNAL OF HEAT TRANSFER, TRANS. ASME, Series C, Vol. 89, No. 4, Nov. 1967, pp. 295–299.

11 Thomas, L. J., and Westwater, J. W., "Microscopic Study of Solid-Liquid Interfaces During Melting and Freezing," *Chem. Engr. Prog. Symp. Series*, Vol. 59, No. 41, 1963, pp. 155–164.

12 Heitz, W. L., "Hydrodynamic Stability of Water and Its Effect on Melting and Freezing," PhD thesis, Univ. of Illinois, Urbana, Ill., 1970.

13 Westwater, J. W., and Heitz, W. L., "Heat Transfer Modes to Confined Water Heated from Below," motion picture, Univ. of Illinois, Urbana, Ill., 1970.

14 Boger, D. V., and Westwater, J. W., "Effect of Buoyancy on the Melting and Freezing Process," JOURNAL OF HEAT TRANSFER, TRANS. ASME, Series C, Vol. 89, No. 1, Feb. 1967, pp. 81–89.

15 Charlson, G. S., "Thermoconvective Instability in a Bounded Cylindrical Fluid Layer," MS thesis, directed by R. L. Sani, Univ. of Illinois, Urbana, Ill., 1969.

16 Yen, Y. C., "Onset of Convection in a Layer of Water Formed by Melting Ice from Below," *Phys. Fluids*, Vol. 11, No. 6, 1968, pp. 1263–1270.

17 Tien, C., "Thermal Instability of a Horizontal Layer of Water Near 4°C," *AIChE Journal*, Vol. 14, No. 4, 1968, pp. 652–653.